

Cholesterol Modulates the Rate and Mechanism of Acetylcholine Receptor Internalization^{*S}

Received for publication, December 13, 2010, and in revised form, February 11, 2011. Published, JBC Papers in Press, February 28, 2011, DOI 10.1074/jbc.M110.211870

Virginia Borroni and Francisco J. Barrantes¹

From the UNESCO Chair of Biophysics and Molecular Neurobiology, Instituto Investigaciones Bioquímicas de Bahía Blanca, C Carrindanga Km 7, B8000FWB Bahía Blanca, Argentina

Stability of the nicotinic acetylcholine receptor (AChR) at the cell surface is key to the correct functioning of the cholinergic synapse. Cholesterol (Chol) is necessary for homeostasis of AChR levels at the plasmalemma and for ion translocation. Here we characterize the endocytic pathway followed by muscle-type AChR in Chol-depleted cells (Chol⁻). Under such conditions, the AChR is internalized by a ligand-, clathrin-, and dynamin-independent mechanism. Expression of a dominant negative form of the small GTPase Rac1, Rac1N17, abolishes receptor endocytosis. Unlike the endocytic pathway in control CHO cells (1), accelerated AChR internalization proceeds even upon disruption of the actin cytoskeleton. Under Chol⁻ conditions, AChR internalization is furthermore found to require the activity of Arf6 and its effectors Rac1 and phospholipase D. The Arf6-dependent mechanism may constitute the default endocytic pathway followed by the AChR in the absence of external ligands, membrane Chol levels acting as a key homeostatic regulator of cell surface receptor levels.

The nicotinic acetylcholine receptor (AChR),² the best characterized member of the Cys loop family within the ligand-gated ion channel superfamily, is an integral membrane protein composed of five homologous subunits organized pseudosymmetrically around a central pore (2). Each subunit contains a relatively large extracellular domain and four hydrophobic transmembrane segments (M1–M4) connected by loops of varying length and ends with a short extracellular carboxyl terminal domain. Three concentric rings can be distinguished in the AChR transmembrane region (3). The M2 transmembrane segments of all subunits outline the inner ring and form the walls of the ion channel proper; M1 and M3 constitute the middle ring, and the M4 segments form the outer ring, which is in closer contact with the AChR lipid microenvironment (4). Early studies demonstrated that the function of AChR depends on the immediate lipid environment and specific interactions

between membrane protein and lipid molecules. These interactions are purported to be responsible for the maintenance of specific secondary structures required to support the ion channel activity of the AChR (5).

AChR internalization in the CHO-K1/A5 clonal cell line and C2C12 muscle cells was recently reported to occur via a novel endocytic mechanism (1) that does not involve the canonical dynamin, clathrin, or caveolin pathways (6). This pathway is triggered by ligand binding to the receptor and requires the activity of the small GTPase Rac1 as well as the integrity of the cytoskeleton. Ligand binding to AChR induces autophosphorylation of c-Src kinase with the consequent activation of Rac1 (1). AChR internalization was also triggered by antibody binding (1), thus relating the internalization process to other pathological conditions, such as those operative in the autoimmune disease myasthenia gravis (7, 8).

We have recently found that cholesterol (Chol), an endogenous lipid present at the postsynaptic membrane, contributes to the homeostasis of receptor levels at the plasmalemma (9, 10). Chol has been found to be necessary for the formation and maintenance of AChR clusters; Chol depletion induces the fragmentation of these relatively large, micrometer sized AChR assemblies (11–14). Likewise, the supramolecular organization of the AChR is influenced by Chol levels; Chol depletion increases the dimensions of AChR nanometer sized clusters and changes the long range distribution of nanoclusters at the cell surface (15). Acceleration of the endocytic internalization of cell surface AChR by Chol depletion (10) is unusual in that all known endocytic mechanisms are hindered upon diminution of cellular Chol levels (6). In the present work, we characterize this unusual modulatory effect induced by Chol on cell surface AChR endocytosis. The endocytic mechanism disclosed here consists of the internalization of receptors via a pathway involving the activity of the small GTPase Arf6 and its effectors Rac1 and phospholipase D but independent of the integrity of the actin network.

EXPERIMENTAL PROCEDURES

Materials—Methyl- β -cyclodextrin (CDx), nystatin, latrunculin A, and cytochalasin D were purchased from Sigma. Alexa Fluor-labeled α BTX and Alexa Fluor-labeled antibodies were purchased from Molecular Probes, Inc. (Eugene, OR) or Invitrogen. mAb210 antibody against the main immunogenic region of the α subunit was a gift from Dr. J. Lindstrom (University of Pennsylvania Medical Center, Philadelphia, PA). Lipofectamine was from Invitrogen. The plasmid coding for dynK44A-HA was provided by S. Schmid (Scripps Research

* This work was supported in part by Ministry of Science and Technology Grants PICT 01-12790 and 5-20155, Argentine Scientific Research Council (Consejo Nacional de Investigaciones Científicas y Técnicas) Grant PIP 6367, Philip Morris USA Inc., and Philip Morris International (to F. J. B.).

^S The on-line version of this article (available at <http://www.jbc.org>) contains supplemental Figs. 1–3.

¹ To whom correspondence should be addressed. E-mail: rtfjb1@criba.edu.ar. Tel.: 54-291-4861201; Fax: 54-291-4861200.

² The abbreviations used are: AChR, acetylcholine receptor; Chol, cholesterol; CDx, methyl- β -cyclodextrin; fPEG-Chol, ester of polyethylene glycol-derivatized cholesterol; PA, phosphatidic acid; PLD, phospholipase D; α BTX, α -bungarotoxin.

Institute). Arf6T27N-HA, Arf6Q67L-HA, and Eps15 Δ 95–295-EGFP were provided by Dr. T. Kirchhausen (Harvard Medical School, Boston, MA). Rac1 N17-HA was a gift from Dr. R. Massol (Children's Hospital, Harvard Medical School). Jaspilakolide was from Calbiochem. The ester of polyethylene glycol-derivatized cholesterol (fPEG-Chol) was provided by Prof. T. Kobayashi (Lipid Biology Laboratory, RIKEN Institute of Physical and Chemical Research, Discovery Research Institute, Saitama, Japan). Rapsyn-GFP was provided by Dr. J. Cohen (Harvard Medical School). None of the plasmids listed affected AChR internalization in cells with normal Chol levels over the period studied (supplemental Fig. 1). Fluorescence transferring and plasmids coding for Rab5-GFP and Rab7-GFP were kindly provided by Dr. J. L. Daniotti (CIQUIBIC, Cordoba, Argentina).

Cell Culture—CHO-K1/A5 cells were grown in Ham's F-12 medium supplemented with 10% fetal bovine serum (FBS) for 2–3 days at 37 °C as described previously (16).

Transient Transfections—In some experiments, CHO-K1/A5 cells were transiently transfected using Lipofectamine according to the protocol provided by the manufacturer. Cells were used for fluorescence microscopy 12 h after transfection.

Acute Chol Depletion/Replenishment of Cultured Cells—CHO-K1/A5 cells were treated with CDx in medium 1 (140 mM NaCl, 1 mM CaCl₂, 1 mM MgCl₂, and 5 mM KCl in 20 mM HEPES buffer, pH 7.4) for 30 min at 37 °C to acutely deplete their Chol content prior to fluorescent labeling as described previously (10). Except for Fig. 1, all experiments were carried out using a final concentration of 15 mM CDx. For Chol replenishment, CDx-Chol complexes were prepared as in Ref. 17. CHO-K1/A5 cells were incubated with 15 mM Chol-CDx complexes (CDx/Chol ratio 6:1) at 37 °C for 30 min.

Biochemical Assays—Lipids were extracted from cell suspensions for 3 h at room temperature in chloroform/methanol/water (1:2:0.8 by volume) following the procedure of Bligh and Dyer (18). Chol determination was carried out using the colorimetric Colestat kit (Wiener Laboratories, Rosario, Argentina).

Disruption/Stabilization of Actin Meshwork—Cytochalasin D stock solution was made in DMSO, and working solutions were prepared upon dilution of the stock in medium 1. The amount of DMSO was kept below 0.5% (v/v). In order to disrupt the cytoskeletal meshwork, CHO-K1/A5 cells were incubated with 12.5 μ M latrunculin A, 2.5 μ M cytochalasin D, or 1 μ M jaspilakolide together with 15 mM CDx. Treatment of control cells with similar amounts of DMSO did not show alteration of cellular morphology or receptor internalization kinetics (see Fig. 3).

Wide Field Fluorescence Microscopy—Cell surface AChR labeling was carried out by incubating the cells in fluorescent α BTX for 1 h in chilled medium 1 on ice. The cells were then examined with a Nikon Eclipse E-600 microscope. Imaging was done with an SBIG Astronomical Instruments (Santa Barbara, CA) model ST-7 digital charge-coupled device camera (765 \times 510 pixels, 9.0 \times 9.0- μ m pixel size). The ST-7 CCD camera was driven by the CCDOPS software package (version 5.02, SBIG Astronomical Instruments). For all experiments, \times 40 (1.0 numerical aperture) or \times 60 (1.4 numerical aperture) oil immersion objectives were used. Appropriate dichroic and

emission filters were employed to avoid cross-over of fluorescence emission. Eight-bit or 16-bit TIFF images were exported for further off-line analysis.

Confocal Microscopy—Cells initially labeled with fluorescent α BTX for 1 h at 4 °C were shifted to 37 °C for 30 min in the presence of CDx or medium 1, respectively. Confocal images were obtained with a TCS-SP2 confocal microscope (Leica Mikrosysteme Vertrieb GmbH, Wetzlar, Germany) equipped with an acousto-optical beam splitter.

Quantitative Image Analysis—Fluorescence intensities of the 8- or 16-bit image were analyzed after manually outlining regions of interest with the software ImageJ (National Institutes of Health, Bethesda, MD). The average fluorescence intensity of a given region of interest was measured within the α BTX-positive region of the cell, and the average fluorescence intensity of an area of the same size positioned over an α BTX-negative region outside the cell was subtracted. The measurements for each experimental condition were undertaken on randomly chosen cells, selected from phase-contrast images to avoid bias. For illustration purposes, images were processed using Adobe Photoshop, scaled with identical parameters, and pseudocolored according to a custom designed look-up table.

RESULTS

AChR Endocytosis Is Accelerated by Disruption of AChR/Chol Interactions and Is Independent of Cholinergic Ligand or Antibody Binding—Chol content was shown to modulate cell surface AChR levels in the CHO-K1/A5 cell line that heterologously expresses adult muscle-type receptor (10). Chol depletion (Chol⁻) of these cells with CDx for 30 min at 37 °C accelerates the internalization of AChR in a dose-dependent manner (Fig. 1, A and B). This acceleration was abolished when cells were enriched in Chol by treatment with 15 mM CDx-Chol complexes for the same period (Fig. 1). In order to verify whether CDx or its complex with Chol did in fact modify cell membrane Chol content, we monitored changes in the fluorescence of the fluorescent Chol analog fPEG-Chol after treatment with CDx or Chol-CDx. fPEG-Chol is a soluble derivative of Chol that preferentially partitions into Chol-rich membrane domains, thus acting as a Chol sensor in cells (19). The fluorescent Chol derivative showed the same cell surface pattern as Alexa Fluor⁶⁴⁷- α BTX. Chol⁻ cells exhibited a marked decrease in cell surface fPEG-Chol fluorescence, and, conversely, an overshoot in fPEG-Chol signal was observed when cells were treated with Chol-CDx (Fig. 1, A and B).

It was previously reported that AChR internalization can be induced by agonists (20), antagonist (1), and antibody binding (21–23). Ligand-triggered endocytosis is a sluggish process in CHO cells, occurring in a time course of hours (10). No internalization of AChR- α BTX complexes is observed within the 30 min time window (Fig. 1C). The effect of CDx treatment was observed when cells were labeled with α BTX before (Fig. 1C) or after (Fig. 1, A and B) Chol depletion. The same result was obtained when cells were exposed to the full nicotinic agonist carbamoylcholine (Fig. 1C, *carb*) during CDx treatment, indicating that the Chol-associated acceleration of AChR internalization is independent of ligand (the agonist carbamoylcholine or the antagonist α BTX) binding. To further corroborate this

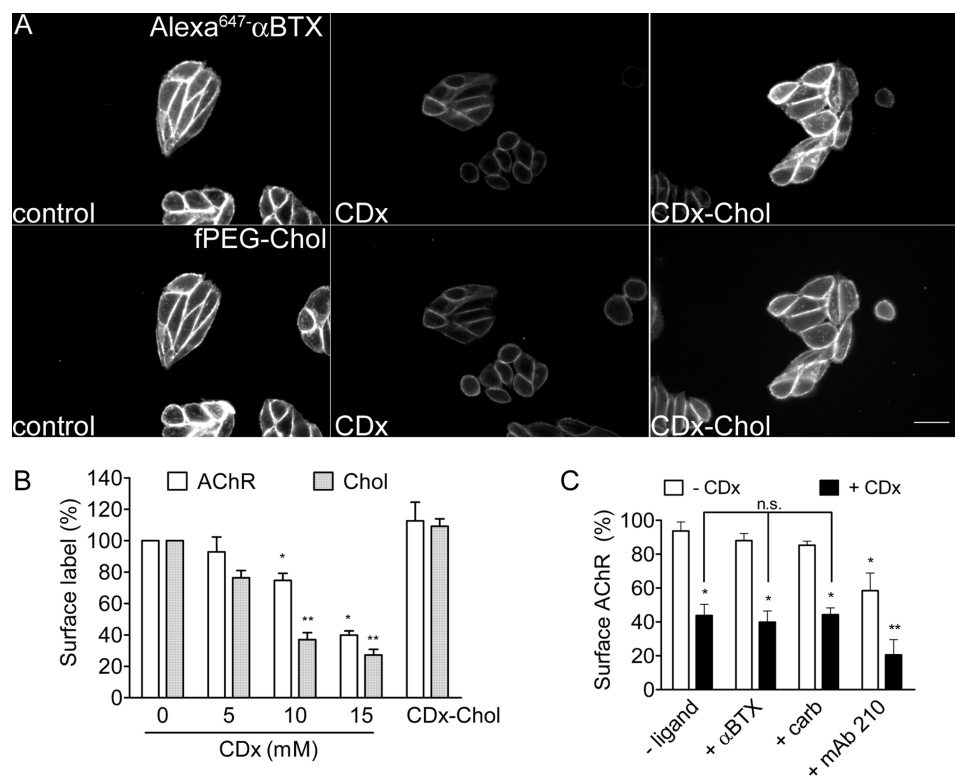


FIGURE 1. Chol depletion accelerates AChR internalization in a ligand- or antibody-independent manner. A, cells were exposed to 15 mM CDx or 15 mM Chol-CDx for 30 min at 37 °C, labeled at the end of the incubation at 4 °C with Alexa Fluor⁶⁴⁷-αBTX (top) and fPEG-Chol (bottom), and imaged. Scale bar, 50 μm. B, cells were exposed to concentrations of 0, 5, 10, or 15 mM CDx or 15 mM Chol-CDx for 30 min at 37 °C, labeled at the end of the incubation at 4 °C with Alexa Fluor⁶⁴⁷-αBTX (empty bars) and fPEG-Chol (gray bars), and imaged. Surface fluorescence was quantified and normalized to that of cells not incubated at 37 °C. *, $p < 0.005$; **, $p < 0.001$ ($n = 4$). An average of 70 cells/condition were analyzed in each experiment. C, cells were labeled with αBTX, carbamoylcholine (carb), or mAb210 monoclonal antibody followed by incubation with (black bars) or without (empty bars) 15 mM CDx for 30 min at 37 °C. At the end of the incubation period, surface AChRs were revealed with antibody staining and imaged. Surface fluorescence was quantified and normalized to that of cells not incubated at 37 °C. n.s., not significant; *, $p < 0.005$; **, $p < 0.001$ from the corresponding control ($n = 4$; an average of 80 cells/condition were analyzed in each experiment). Error bars, S.D.

observation, we labeled AChR with the specific antibody mAb210, which binds to the main immunogenic region of the AChR α subunit. As shown in Fig. 1C, AChR internalization is triggered by mAb210 binding (Fig. 1C). Chol depletion has an *additive* effect (Fig. 1C). This series of experiments indicates that Chol depletion accelerates AChR internalization in a ligand- and antibody-independent manner.

Acceleration of AChR Endocytosis Is Reversible and Involves the Disruption of AChR/Chol Interactions—In order to test the reversibility of the effect of Chol depletion on AChR internalization, cells were first depleted of Chol and, immediately after, replenished with Chol using Chol-CDx complexes. At the end of the incubation period, we monitored the changes in AChR and Chol surface levels (Fig. 2A) as well as the total cellular Chol content (Fig. 2B). As shown above, surface AChR levels decreased when Chol was removed from the membrane (Fig. 1A and Fig. 2A, CDx). However, within the time period studied, internalized AChR did not return to the cell surface even upon restoring Chol levels (Fig. 2, A and B, CDx/CDx-Chol). It is worth noting that cells recover *membrane* Chol, whereas the level of *total* Chol remains low (Fig. 2, A and B, CDx/F12). When cell membrane Chol returns to control levels (Fig. 2A, CDx/F12 and CDx/CDx-Chol), AChR is no longer internalized at an accelerated rate (Fig. 2A, CDx/F12 and CDx/CDx-Chol), suggesting that *surface membrane* Chol is the determining fac-

tor that modulates plasmalemmal AChR independently of the total Chol content of the cell. To further test this hypothesis, an additional experiment was devised to specifically affect the availability of Chol at the cell surface. Unlike CDx, the CDx surrogate, nystatin, an antibiotic that binds to and forms complexes with membrane-bound Chol, sequesters the neutral lipid without removing it from the membrane (24). When cells were treated with 50 μg/ml nystatin for 1 h at 37 °C, a ~25% diminution of cell surface AChR was observed (Fig. 2C). As expected, fPEG-Chol levels were not affected (Fig. 2C). Treatment of CHO-K1/A5 cells with nystatin also resulted in the loss of surface AChR, although its effect was less apparent than in the case of CDx. This series of experiments indicates that membrane Chol is necessary for AChR stability and that it is the disruption of AChR-Chol interactions rather than the physical removal of Chol from the membrane that accelerates AChR endocytosis.

Relationship between AChR Accelerated Internalization Induced by CDx and the Actin Cytoskeleton—CDx treatment has been reported to augment the stability of the submembrane cytoskeleton and in particular the actin meshwork (25). Previous work from our laboratory showed that AChR nanoclusters (<50 nm in diameter) were randomly distributed at the cell membrane but acquired long range (within a 0.25–1.5-μm radius) order upon Chol depletion (15). These observations led

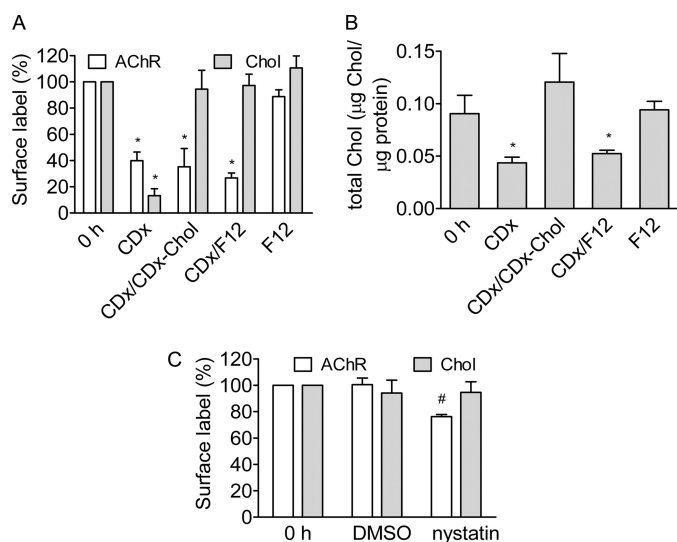


FIGURE 2. Membrane Chol depletion accelerates AChR internalization. A, cells were incubated with 15 mM CDx for 30 min at 37 °C and immediately after with CDx-Chol (CDx/CDx-Chol) or Ham's F-12 medium (CDx/F12). As controls, cells were not incubated at 37 °C (0 h) and were incubated only with 15 mM CDx for 30 min at 37 °C (CDx) or with F-12 for 1 h at 37 °C (F12). At the end of the incubation period, cells were labeled with Alexa Fluor⁶⁴⁷-αBTX and fPEG-Chol at 4 °C and imaged. Surface levels of AChR (empty bars) and Chol (gray bars) were calculated and normalized to that of cells not incubated at 37 °C. Another set of cells were treated as above and at the end of the incubation were suspended in PBS in order to perform the extraction of lipids according to Bligh and Dyer. Total Chol (B) was determined as described under "Experimental Procedures." *, statistically significant differences from control cells (0 h) with $p < 0.001$ ($n =$ at least 3 independent experiments). C, cells were treated for 1 h at 37 °C with 50 μg/ml nystatin or the equivalent amount of DMSO and at the end of the incubation were labeled at 4 °C with Alexa Fluor⁶⁴⁷-αBTX and fPEG-Chol and imaged. Surface fluorescence was quantified and normalized to that of cells not incubated at 37 °C (0 h). #, $p < 0.01$ ($n = 3$). Error bars, S.D.

us to speculate on the possible involvement of the cytoskeletal meshwork in this process and prompted us to investigate whether the acceleration of AChR endocytosis under Chol⁻ conditions was associated with actin meshwork reorganization. Cells were co-incubated for 30 min at 37 °C with CDx (15 mM) and drugs that inhibit actin polymerization: latrunculin A (12.5 μM), cytochalasin D (2.5 μM) (26, 27), or jasplakinolide (1 μM), a drug that promotes actin polymerization (28, 29). None of these drugs by themselves exerted any effect on AChR internalization in Chol-depleted cells over the 30-min period tested here. When stained with rhodamine-labeled phalloidin, a probe of filamentous actin, control cells exhibited the characteristic pattern of actin stress fibers, some immediately adjacent to the cell membrane. The corresponding Alexa Fluor⁶⁴⁷-αBTX fluorescence was observed only at the cell surface in proximity to the actin stress fibers. Upon treatment of cells with CDx (together with the solvent used for all drugs in this series of experiments, DMSO) Alexa Fluor⁶⁴⁷-αBTX staining was observed in the form of punctuate structures, compatible with endosomes. Internalized AChRs thus lost any proximity relationship with the actin fibers (Fig. 3A). When Chol depletion occurred in the presence of cytochalasin D, actin stress fibers decreased in number and clumped together noticeably, but AChR internalization was not affected (Fig. 3A). Treatment with 12.5 μM latrunculin A produced a massive disruption of the stress fibers, phalloidin staining became punctiform, and cells rounded up

(Fig. 3A), but AChR endocytosis proceeded as in control cells (Fig. 3B). As expected, when cells were treated with jasplakinolide, a drug that induces polymerization of monomeric actin into amorphous masses (28), actin did not stain with the fluorescent phalloidin because the two molecules compete for the same binding site on actin fibers (Fig. 2A). Thus, cells treated with CDx together with latrunculin A, cytochalasin D, or jasplakinolide showed the same pattern of AChR internalization as cells treated with CDx alone (Fig. 3A). They also showed the same reduction in AChR surface levels (Fig. 3B), indicating that when cellular Chol levels are reduced, AChR internalization no longer depends on the integrity of the actin cytoskeleton.

The presence of accessory receptor-binding proteins in muscle cells, such as rapsyn, increases the stability of the AChR in the membrane (30–34). Rapsyn is associated with the AChR in a 1:1 stoichiometry and stabilizes the receptor protein by linking it with the cytoskeleton (33, 35, 36). Because CHO-K1/A5 cells lack rapsyn, it was necessary to discard the possibility that it is the absence of this protein that makes AChR endocytosis sensitive to Chol levels. In order to test this hypothesis, CHO-K1-A5 cells were transfected with a plasmid coding for rapsyn-GFP, and AChR internalization was followed in Chol-depleted cells. Rapsyn-expressing cells (marked with an asterisk in supplemental Fig. 2) showed the same pattern of internalization as control cells. Moreover, the presence of rapsyn did not alter the number of cells that internalized AChRs when treated with CDx (supplemental Fig. 2). These results indicate that the absence of the non-receptor protein rapsyn in CHO cells is not responsible for the sensitivity of AChR internalization to Chol levels.

Internalized AChR Is Transported to Specific Endosomes— Upon Chol depletion, AChR·αBTX complexes were internalized much faster. To elucidate the nature of the structures intervening in AChR endocytosis under Chol⁻ conditions, we performed co-localization studies with markers of different subcellular compartments. Cells were transiently transfected with plasmids coding for the early endosome marker Rab5-GFP or the late endosome marker Rab7-GFP. Twelve h after transfection, cells were labeled with Alexa Fluor⁶⁴⁷-αBTX for 1 h at 4 °C, washed with medium 1, and treated with 15 mM CDx for 30 min at 37 °C. At the end of the incubation period, cells were imaged. Some αBTX-AChR labeled endosomes were found to co-localize with Rab5-GFP and Rab7-GFP (Fig. 4, top), making it apparent that the receptor-ligand complex is targeted to an endosomal compartment. αBTX-AChR-labeled endosomes do not colocalize with the lysosome marker LysoTracker during the 30-min incubation, indicating that there is no AChR degradation over this period; no reduction in total AChR levels was observed in Chol⁻ cells up to 1 h (Fig. 4, histogram). AChR·αBTX complexes colocalize with lysosome markers only after this 1-h period (Fig. 4, middle), suggesting that internalized AChRs are targeted to degradation. Once internalized, AChR-containing endosomes do not colocalize with fluorescent transferrin or FITC-dextran over the 30-min incubation period, implying that the entry route followed by AChR in Chol⁻ cells does not overlap with the clathrin- and Cdc42-dependent pathways (Fig. 4, bottom).

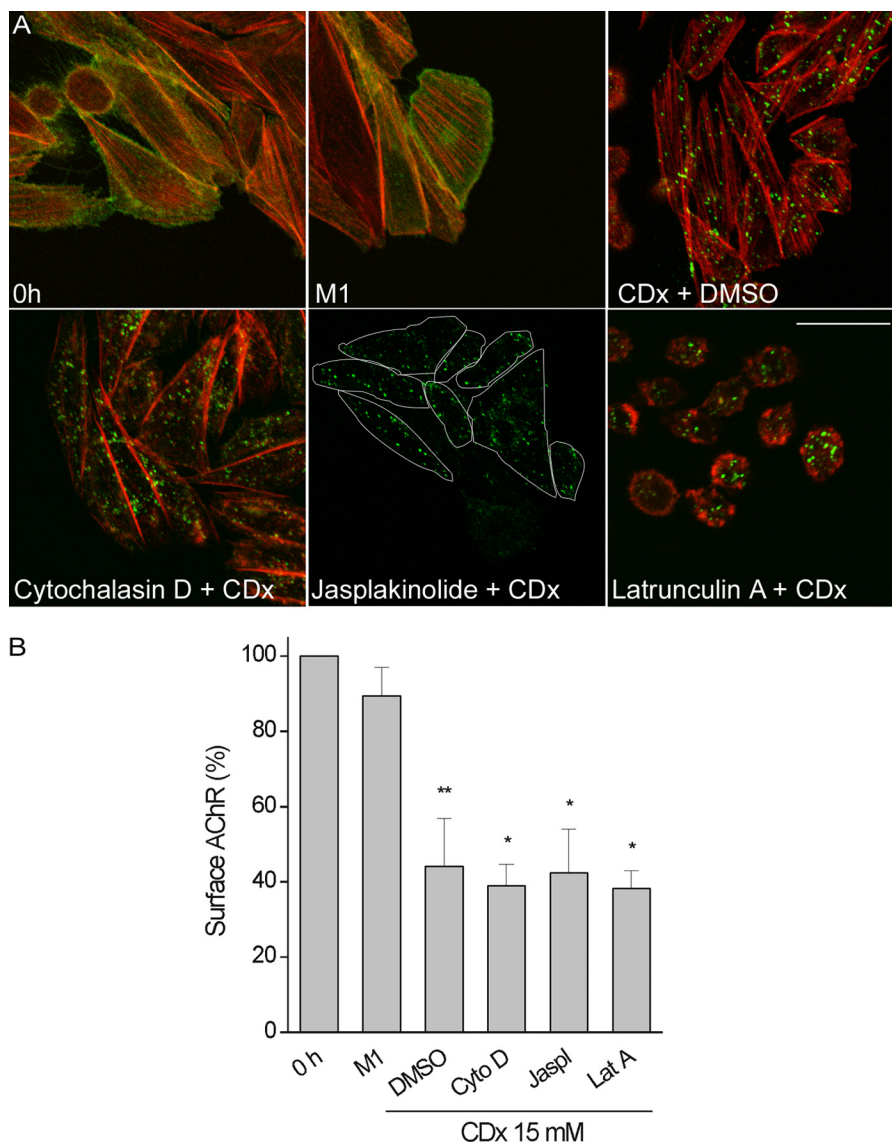


FIGURE 3. AChR internalization induced by Chol depletion is independent of cytoskeleton rearrangement. *A*, cells were labeled with Alexa Fluor⁶⁴⁷- α BTX (pseudocolored in green in the images) at 4 °C for 1 h and subsequently incubated for 30 min at 37 °C in medium 1 containing 15 mM CDx and 0.06% DMSO, 2.5 μ M cytochalasin D plus 15 mM CDx, 1 μ M jasplakinolide plus 15 mM CDx, or 12.5 μ M latrunculin A plus 15 mM CDx. At the end of the incubation, cells were fixed, permeabilized, and incubated with rhodamine-labeled phalloidin (red in the images) and imaged. Scale bar, 20 μ m. *B*, cells were incubated for 30 min at 37 °C in medium 1, 15 mM CDx plus DMSO (DMSO); cytochalasin D plus 15 mM CDx (Cyto D); jasplakinolide plus 15 mM CDx (Jaspl); or latrunculin A plus 15 mM CDx (Lat A). At the end of the incubation period, cells were labeled with Alexa Fluor⁴⁸⁸- α BTX for 1 h at 4 °C and imaged. Fluorescence intensity of cells was quantified and data were normalized to the fluorescence intensity of cells not incubated at 37 °C (0 h). The histogram represents mean \pm S.D. (error bars). *, $p < 0.001$; **, $p < 0.005$ ($n = 3$; an average of 70 cells/condition were analyzed in each experiment).

Upon Chol Depletion, AChR Internalization Remains Independent of the Canonical Clathrin- and Dynamin-dependent Pathways—In order to characterize the mechanism underlying the acceleration of cell surface AChR upon Chol depletion from the membrane, CHO-K1/A5 cells were transiently transfected with the cDNA coding for a dominant negative mutant of dynamin (dynK44A-HA) and a truncated form of Eps15, Eps15 Δ 95–295-EGFP, which blocks entry of cargo through the clathrin pathway (37, 38). As shown previously in cells having normal Chol levels (1), neither dynK44A-HA nor Eps15 Δ 95–295-EGFP expression affected AChR internalization; however, as expected, internalization of fluorescent transferrin was impaired in cells transfected with either plasmid (supplemental Fig. 3). Twelve h after transfection, cells were labeled with Alexa

Fluor⁶⁴⁷- α BTX at 4 °C and submitted to CDx treatment. Transfected cells were identified by EGFP fluorescence in the case of Eps15 Δ 95–295-EGFP and by HA antigen immunocytochemistry in the case of dynK44A-HA. As shown in Fig. 5, neither Eps15 Δ 95–295-EGFP nor dynK44A-HA overexpression affected the internalization of AChR induced by Chol depletion, indicating that the accelerated AChR internalization in the Chol⁻ condition does not proceed via the clathrin- or dynamin-dependent mechanisms previously disclosed (1).

CDx-mediated Acceleration of AChR Endocytosis Depends on the Small GTPase Arf6—Arf6 is a member of the Arf (ADP-ribosylation factor) family of GTP-binding proteins. It is localized at the plasma membrane, where it regulates membrane traffic (39). A clathrin-independent endocytic pathway associ-

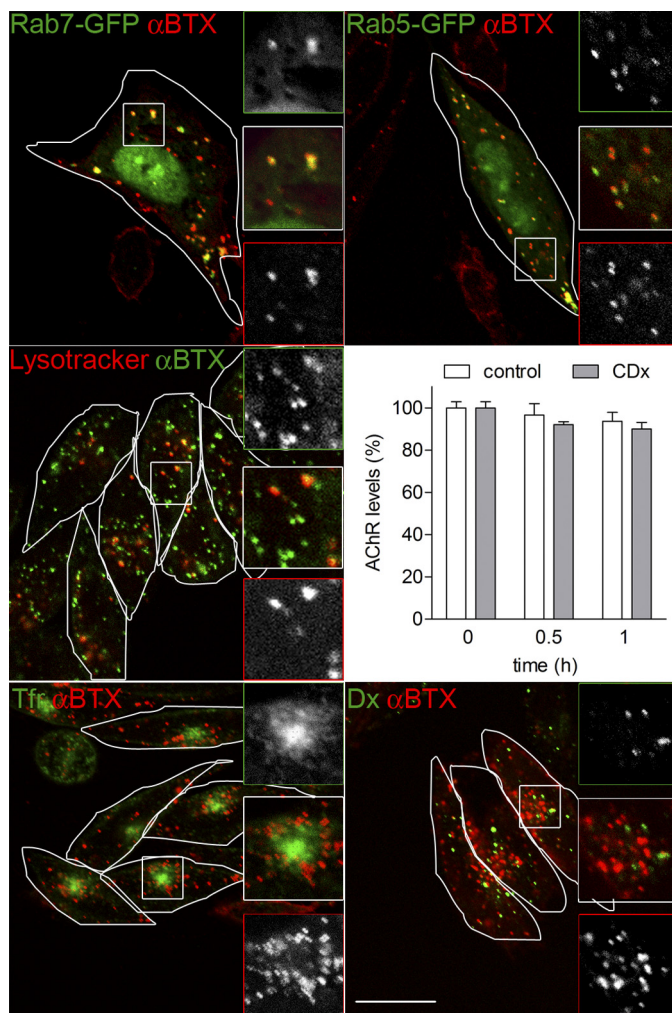


FIGURE 4. Internalized AChR is transported to specific endosomes. *Top*, cells transiently transfected with plasmids coding for Rab7-GFP or Rab5-GFP (green in the images) were labeled with Alexa Fluor⁶⁴⁷-αBTX (shown in red in the images) for 1 h at 4 °C, washed with medium 1, and incubated with 15 mM CDx at 37 °C. At the end of the incubation period, cells were imaged by confocal microscopy. Scale bar, 20 μm (10 μm in the inset). *Middle*, cells were labeled with Alexa Fluor⁶⁴⁷-αBTX (shown in red in the images) for 1 h at 4 °C, washed with medium 1, and incubated with 15 mM CDx at 37 °C in the presence of LysoTracker (green in the images). At the end of the incubation period, cells were imaged by confocal microscopy. Scale bar, 20 μm (10 μm in the inset). Cells were labeled with Alexa Fluor⁴⁸⁸-αBTX for 1 h at 4 °C, washed with medium 1, and incubated with 15 mM CDx at 37 °C for 30 min or 1 h. At the end of the incubation period, cells were imaged, and total fluorescence was quantified. The results were normalized against cells treated as before but not incubated at 37 °C. ($n = 3$). *Bottom*, cells were labeled with Alexa Fluor⁴⁸⁸-αBTX or Alexa Fluor⁶⁴⁷-αBTX (red in the image) at 4 °C and then shifted to 37 °C in the presence of 15 mM CDx and Cy5-transferrin (*Tfr*) or FITC-Dx (green in the image). At the end of the incubation period, cells were imaged. Scale bar, 30 μm (15 μm in the inset). Error bars, S.D.

ated with Arf6 has been described (40). The next series of experiments was aimed at establishing whether AChR internalization is affected by Arf6 under Chol⁻ conditions. CHO-K1/A5 cells were transiently transfected with a dominant negative (Arf6T27N-HA) or a constitutively active mutant (Arf6Q67L-HA) of Arf6 and submitted to CDx treatment. Overexpression of the Arf6 dominant negative mutant (Arf6T27N-HA) clearly inhibited the acceleration of AChR internalization kinetics typically observed upon Chol depletion. The number of cells that showed augmented CDx-mediated

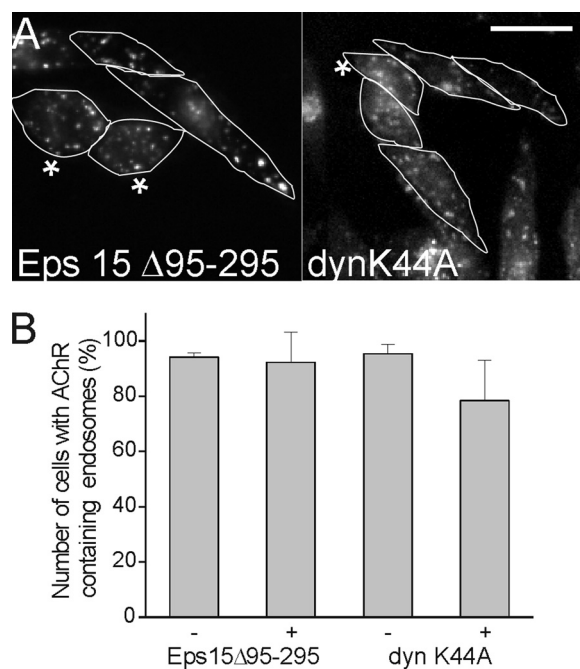


FIGURE 5. AChR internalization induced by Chol depletion does not proceed via clathrin- or dynamin-dependent mechanisms. *A*, cells were transiently transfected with plasmids coding for a truncated form of Eps15, Eps15Δ95–295-EGFP, or a dominant negative mutant of dyn (dynK44A-HA). Transfected cells were labeled at 4 °C with Alexa Fluor⁶⁴⁷-αBTX and submitted to CDx treatment for 30 min at 37 °C. After the incubation period, cells transfected with dynK44A-HA were fixed, permeabilized, and immunostained with antibodies against the HA epitope in order to identify transfected cells. The asterisks indicate transfected cells. Scale bar, 20 μm. *B*, the number of untransfected (–) or transfected (+) cells displaying AChR endosomes was quantified in each case and normalized to the number of cells displaying AChR endosomes in an untransfected dish ($n = 3$; an average of 30 transfected and 50 untransfected cells were analyzed in each experiment). Error bars, S.D.

internalization was more than 50% lower. Further corroborating these findings, cells transfected with the dominant active form of Arf6 (Arf6Q67L-HA) showed the same behavior as control cells, indicating that the above results are not an artifact of overexpression (Fig. 6A).

In order to evaluate the effect of Arf6 inhibition in more detail, we performed a double labeling protocol. Transfected cells were initially labeled with Alexa Fluor⁵⁶⁸-αBTX (red) at 4 °C and subsequently exposed for 30 min at 37 °C to CDx or medium 1. At the end of the incubation period, cells were labeled with mAb210 anti-AChR antibody and Alexa Fluor⁶⁴⁷-secondary antibody (far red). Cells were then fixed, permeabilized, and labeled with anti-HA antibody and Alexa Fluor⁴⁸⁸-secondary antibody. According to this protocol, red fluorescence represents total AChR present at the cell surface at the beginning of the experiment, and far red fluorescence corresponds to AChR remaining at the surface at the end of the experiment. Changes in the far red/red ratio thus provide a quantitative estimation of the degree of AChR internalization. In cells transfected with Arf6T27N and treated with CDx, only ~20% of the AChRs were internalized, a figure similar to that of cells incubated with medium 1 only (Fig. 6C). This series of experiments provides additional support to the novel observation that CDx enhances the internalization of AChR via an Arf6-dependent mechanism. In contrast, in control cells hav-

Cholesterol Modulation of AChR Endocytosis

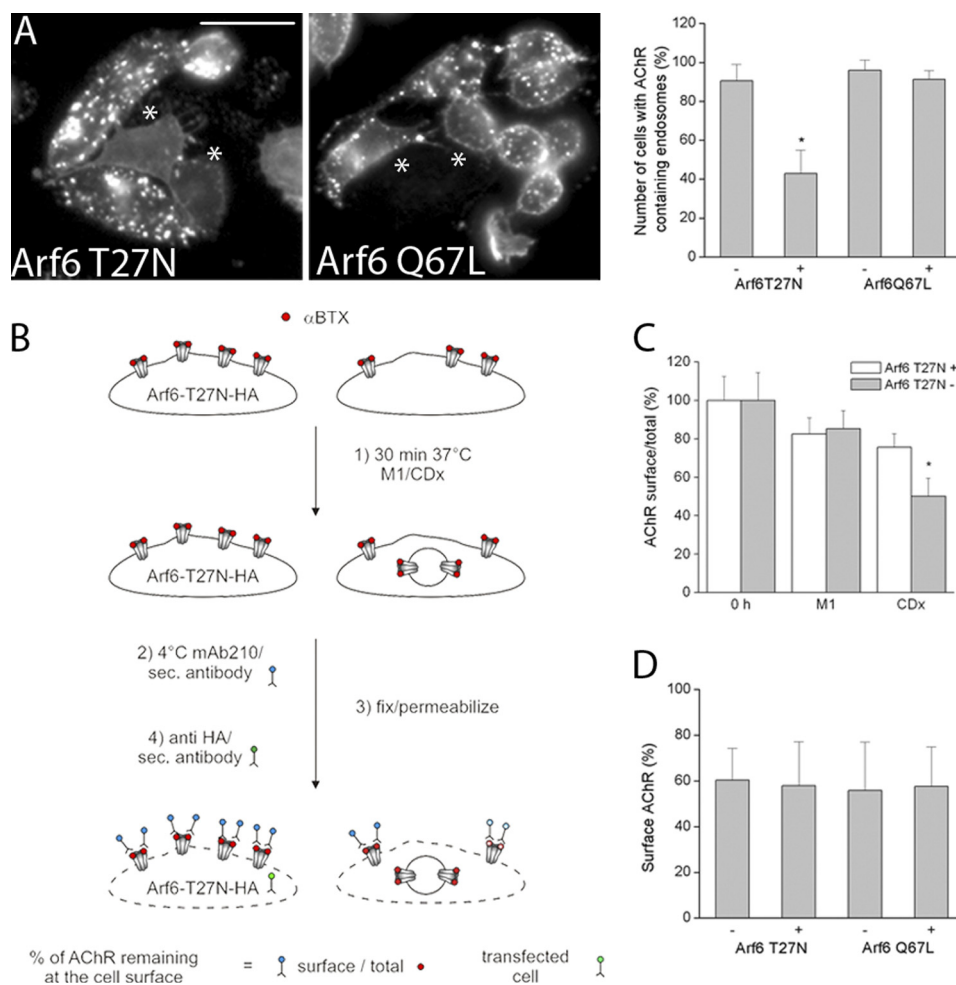


FIGURE 6. Acceleration of AChR internalization mediated by Chol depletion is Arf6-dependent. *A*, cells were transiently transfected with plasmids coding for a dominant negative mutant (Arf6T27N-HA) or a dominant active mutant (Arf6Q67L-HA) of Arf6. Transfected cells were labeled at 4 °C with Alexa Fluor⁶⁴⁷- α BTX and submitted to CDx treatment for 30 min at 37 °C. After the incubation period, cells were fixed, permeabilized, and immunostained with antibodies against the HA epitope in order to identify transfected cells. The *left panel* shows representative images of Alexa Fluor⁶⁴⁷- α BTX fluorescence from cells treated as described above. The *asterisks* indicate transfected cells. *Scale bar*, 20 μ m. The number of untransfected (-) or transfected (+) cells displaying AChR-positive endosomes was quantified in each case and normalized to the number of cells displaying AChR-positive endosomes in an untransfected dish. *, $p < 0.001$ ($n = 5$; an average of 20 transfected and 50 untransfected cells were analyzed in each experiment). *B*, schematic diagram depicting the experimental protocol followed to test the effect of the dominant negative Arf6 mutant. Cells were transfected with the plasmid coding for Arf6T27N-HA, labeled with AlexaFluor⁵⁶⁸- α BTX (red dots) at 4 °C, and subsequently exposed to CDx or medium 1, respectively, at 37 °C for 30 min. At the end of the incubation period, cells were labeled with mAb210 and Alexa Fluor⁶⁴⁷-secondary antibody (blue dots). Cells were then fixed, permeabilized, and labeled with anti-HA antibody and Alexa Fluor⁴⁸⁸-secondary antibody (green dots). *C*, surface (mAb210/Alexa Fluor⁶⁴⁷-secondary antibody) and total (Alexa Fluor⁵⁶⁸- α BTX) AChR levels were quantified and normalized against $t = 0$ h in transfected (gray bars) and untransfected (empty bars) cells. *, $p < 0.05$ ($n = 3$; an average of 20 transfected and 50 untransfected cells/condition were analyzed in each experiment). *D*, cells transfected with plasmids coding for Arf6T27N-HA or Arf6Q67L-HA were initially labeled with biotin- α BTX at 4 °C and subsequently incubated in growth medium at 37 °C for 6 h. At the end of the incubation period, cells were labeled with Cy5-streptavidin in order to detect AChR remaining at the surface. Cells were then fixed, permeabilized, and immunostained to detect HA epitopes. Surface AChR was quantified and normalized against cells not incubated at 37 °C in transfected (Arf6T27N+ or Arf6Q67L+) and untransfected (Arf6T27N- or Arf6Q67L-) cells. ($n = 3$; an average of 30 transfected and 50 untransfected cells were analyzed in each experiment). *Error bars*, S.D.

ing normal Chol levels, transfection of dominant negative or constitutive active mutants of Arf6 had no effect on AChR internalization even after 6 h of chase (Fig. 6D). Taken together, this series of experiments shows that AChR endocytosis becomes sensitive to Arf6 activity under conditions of low Chol levels.

CDx-mediated Acceleration of AChR Endocytosis Is Dependent on Rac1—Rac1 is another small GTPase that is coupled to Arf6 activation in many cellular events related to membrane trafficking and actin remodeling (41–45). The fact that under Chol⁻ conditions AChR internalization became sensitive to Arf6 activity prompted us to investigate whether Rac1 activity was necessary for the aforementioned phenomenon. To test

this possibility, we transiently transfect CHO-K1/A5 cells with a dominant negative form of Rac1 (Rac1N17-HA) and assayed for AChR endocytosis in control and Chol⁻ cells. As shown in Fig. 7A, a clear reduction was observed in the number of Rac1N17-HA-expressing cells that internalized AChR upon CDx treatment. This result suggests that functional Rac1 is necessary for acceleration of AChR endocytosis under conditions of low Chol levels.

CDx-mediated Acceleration of AChR Endocytosis Is Dependent on Phospholipase D—Arf6 activation is also coupled with the generation of phosphatidic acid (PA) through phospholipase D (PLD)-mediated hydrolysis of phosphatidylcholine. In the context of membrane trafficking, PA is an important lipid

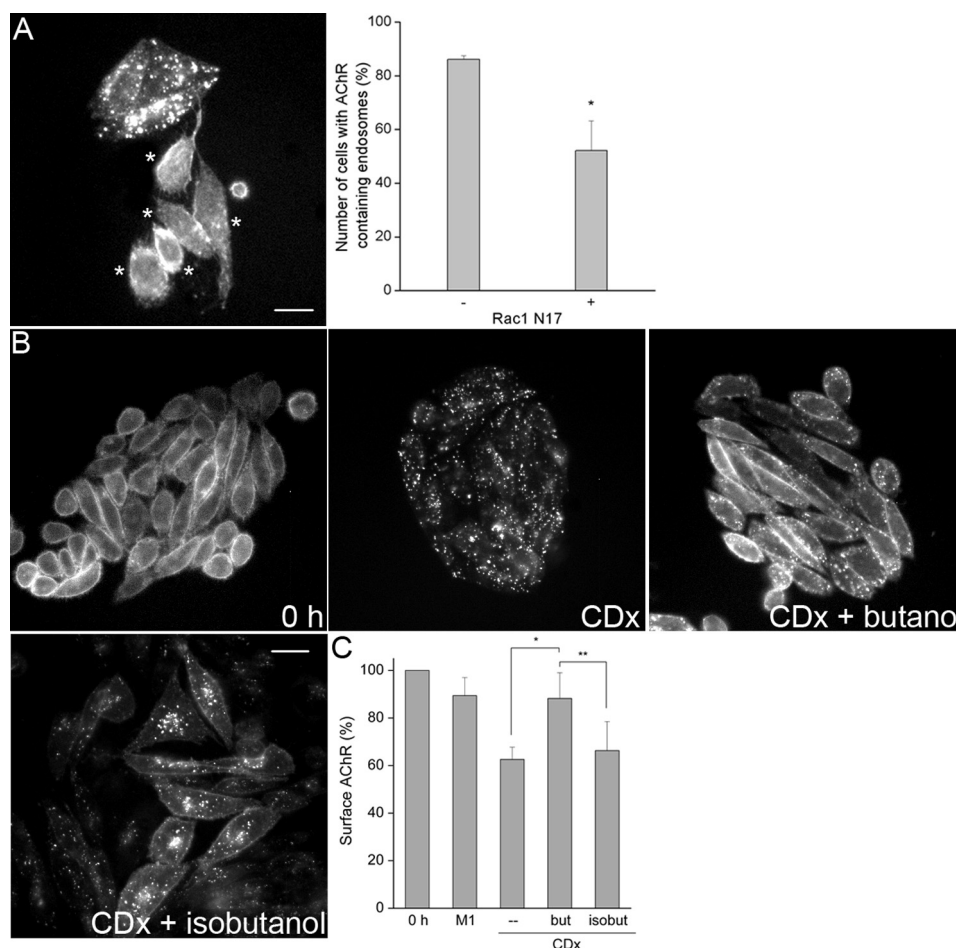


FIGURE 7. The acceleration of AChR internalization induced by Chol depletion depends on Rac1 and PLD. *A*, cells were transiently transfected with a plasmid coding for a dominant negative mutant of Rac1, Rac1N17-HA. Transfected cells were labeled at 4 °C with Alexa Fluor⁶⁴⁷- α BTX and submitted to 15 mM CDx treatment for 30 min at 37 °C. At the end of the incubation period, cells were fixed, permeabilized, and immunostained for the HA epitope in order to identify transfected cells. *Left*, images of Alexa Fluor⁶⁴⁷- α BTX fluorescence from cells treated as described above. The *asterisks* indicate transfected cells. *Scale bar*, 50 μ m. The number of untransfected (–) or transfected (+) cells displaying AChR endosomes was quantified in each case and normalized to the number of cells displaying AChR endosomes in an untransfected dish. *, $p < 0.005$ ($n = 5$; an average of 20 transfected and 50 untransfected cells were analyzed in each experiment). *B*, cells were labeled at 4 °C with Alexa Fluor⁴⁸⁸- α BTX and incubated with 15 mM CDx, 15 mM CDx plus 0.3% 1-butanol, or 15 mM CDx plus 0.3% isobutyl alcohol for 30 min at 37 °C. At the end of the incubation period, cells were imaged. *Scale bar*, 50 μ m. Cells were labeled at 4 °C with biotin- α BTX and incubated with 15 mM CDx, 15 mM CDx plus 0.3% 1-butanol, or 15 mM CDx plus 0.3% isobutyl alcohol (*isobutanol*) for 30 min at 37 °C. At the end of the incubation period, cells were labeled with Alexa Fluor⁴⁸⁸-streptavidin and imaged. Surface fluorescence was quantified in each cell and normalized against surface fluorescence of cells not incubated at 37 °C (0 h). *, $p < 0.01$; **, $p < 0.05$ ($n = 3$; an average of 80 cells/condition were analyzed in each experiment). *Error bars*, S.D.

involved in the formation and fission of vesicles (46, 47). To elucidate whether the internalization of the AChR in Chol[–] cells requires the formation of PA, cells were co-incubated with CDx and 1-butanol. Primary alcohols like 1-butanol shift the generation of PA by PLD to the corresponding phosphatidyl alcohol, which is inactive (48). Alcohols with branched chains, like isobutyl alcohol, are not substrates of PLD and were thus used as controls. As shown in Fig. 7, *B* and *C*, cells treated with CDx and 0.3% 1-butanol showed an inhibition of AChR internalization, concomitant with an increase in AChR surface levels. However, the use of isobutyl alcohol instead of 1-butanol caused no inhibition of AChR internalization (Fig. 7, *B* and *C*).

DISCUSSION

Many steps during the formation of the neuromuscular junction involve changes in the availability of Chol. In a similar manner to when CHO/K1-A5 cells are treated with CDx, mem-

brane cholesterol gradually decreases up to ~45% with the differentiation of C2 cells, such decrease being necessary for myoblast fusion (49). Chol levels are subsequently recovered and become important in both the formation and stabilization of agrin-induced AChR clusters (11–13). In the present work, as in our previous work (10), we dissect the role of Chol in AChR surface stability by reducing membrane cholesterol levels with the cholesterol-depleting agent CDx (50) and membrane Chol availability with the Chol-sequestering agent, nystatin (24). Both approaches accelerated AChR internalization.

AChR cell surface levels are modulated by ligand binding, as shown in various mammalian cell systems as well as in the neuromuscular junction *in vivo* (1, 20, 23, 51). Binding of the competitive antagonist α BTX or antibody-mediated cross-linking triggers the internalization of cell surface AChR in CHO-K1/A5 cells and of endogenous muscle-type AChR in C2C12 myoblasts via a dynamin-, clathrin-, caveolin-, and Arf6- indepen-

Cholesterol Modulation of AChR Endocytosis

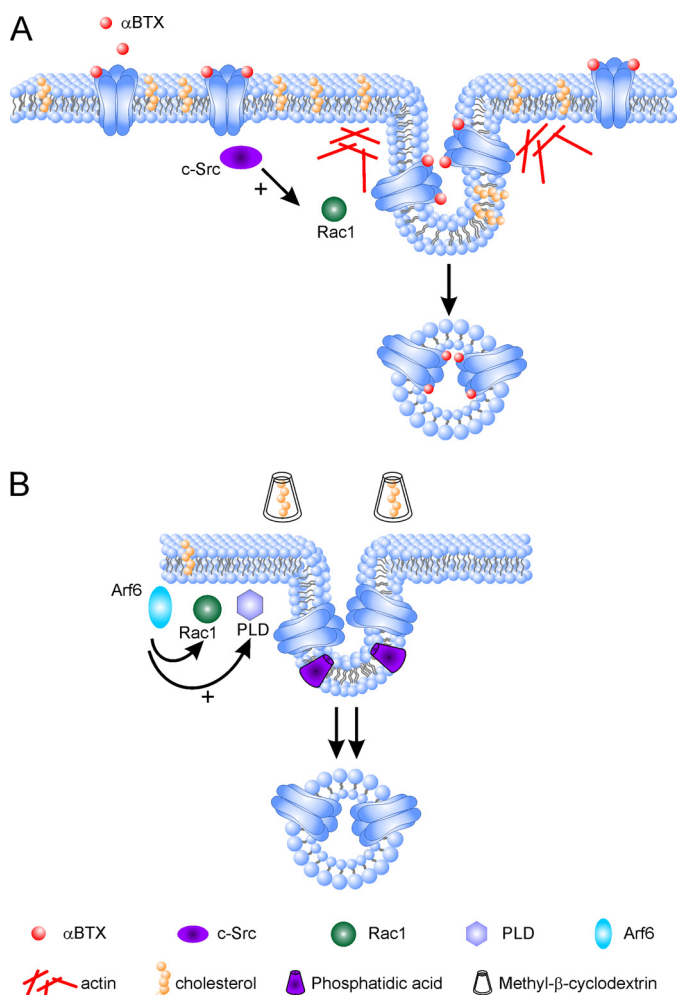


FIGURE 8. Schematic diagram showing the endocytic pathway followed by AChR in cells under normal (A) and low (B) cholesterol levels, respectively. *A*, under control conditions, the AChR is internalized by a pathway triggered by ligand binding to the receptor. Binding activates c-Src kinases, which in turn activate the small GTPase, Rac1. Rac1 GTPase modulates actin dynamics to allow AChR internalization. *B*, when membrane cholesterol levels are reduced or low in comparison with control levels (such as prior to AChR stabilization during myoblast differentiation), AChR internalization is accelerated and no longer depends on ligand binding. Under these conditions, AChR internalization requires the activity of another GTPase, Arf6, and its effectors Rac1 and PLD. Production of phosphatidic acid by PLD may replace cholesterol at the AChR lipid microenvironment and facilitate the formation of endocytic vesicles. Furthermore, the actin cytoskeleton is not coupled to AChR internalization when cholesterol levels are reduced.

dent mechanism (1). This pathway requires the activity of the small GTPase Rac1 and the tyrosine kinase c-Src and the integrity of the cytoskeleton (Fig. 8 and ref. 1). In contrast, as shown here, AChR internalization in Chol^- cells is *independent* of ligand binding; neither prelabeling of cells with the antagonist αBTX nor binding of the agonist carbamoylcholine or the antibody mAb210 is necessary to induce AChR endocytosis in Chol^- cells (Fig. 8). Thus, cholesterol may constitute an endogenous modulator of AChR surface levels of unliganded cell surface receptors at the neuromuscular junction. Conversely, interaction of AChR with Chol in the membrane may confer ligand dependence on AChR internalization.

The consequence of Chol depletion on the rate of AChR internalization is unusual (10); whereas this treatment severely hinders most endocytic pathways, the opposite

effect, acceleration, appears to be operative in the case of AChR internalization in CHO-K1/A5 cells. Several studies have indicated the need for Chol to maintain AChR conformation and function (10). Recent dynamic *in silico* molecular simulations of AChR suggest that the structure collapses in the absence of Chol (52). Hence, Chol depletion could also be associated with changes in AChR conformation, making it more sensitive to internalization.

The effects of Chol depletion on the plasma membrane are diverse and complex (50). CDx treatment has been reported to augment the stability of the actin cytoskeleton, an effect related to the redistribution of phosphatidylinositol 4,5-bisphosphate (25). In CHO-K1/A5 cells with normal Chol levels, AChR internalization *does require* the integrity of the cytoskeleton (1). However, as shown here, when the Chol level is reduced, internalization of AChR proceeds even when the actin cytoskeleton is distressed. Perturbation of actin filaments by cytochalasin D, latrunculin A, or jasplakinolide treatment affected neither the rate of AChR internalization nor the gross morphology of AChR-containing endosomes. These data support the notion that Chol depletion may uncouple actin dynamics from AChR internalization kinetics.

Blocking of Arf6 activity inhibited AChR endocytosis in Chol^- cells. A decrease in the number of cells that internalize AChR and a reduction in the AChR internalization rate were apparent in cells expressing the dominant negative form of Arf6, Arf6T27N. Under normal Chol levels, however, AChR internalization is insensitive to Arf6 activity. No effects were observed with the constitutively active mutant of Arf6, Arf6Q67L. AChR internalization requires activation of the Rho GTPase Rac1, both in Chol^- cells and in cells with normal Chol levels. Blocking Rac1 activity by overexpression of a dominant negative mutant of this protein leads to stabilization of AChRs in Chol^- cells. Rac1 activation therefore appears to be the key (and so far only) common event in AChR internalization, and this activation can be achieved by totally different means: binding of a competitive antagonist like αBTX or anti-AChR antibodies (1) or Chol depletion, as shown here.

There is increasing evidence of the cross-talk between Arf6 and Rac1 signaling (41, 42, 45, 53–55). Chol depletion was shown to activate Rac1 (56), mimicking the effect of loss of adhesion (57, 58). It is interesting to note that cell adhesion to specific extracellular matrix proteins can lead to the formation of complex AChR clusters very similar to those present in the mature neuromuscular junction (59). Formation of large, micrometer sized clusters of AChR is associated with increased AChR stability and requires Chol (11–14). Disruption of lipid domains was shown to destabilize AChR clusters in C2C12 and CHO-K1/A5 cells (10, 12, 13). The intervening mechanism is not clear, although loss of AChR association with rapsyn and changes in the state of AChR phosphorylation have been postulated (12). In the present work, the participation of rapsyn has been ruled out; overexpression of rapsyn-GFP does not affect the accelerated AChR endocytosis in Chol^- cells. Interestingly, although the AChR nanoclusters in CHO cells are much smaller than the fully developed “macroclusters” in the adult muscle synapse, they seem to respond to Chol depletion in a like

manner, suggesting a conserved lipid (Chol) dependence for maintaining AChR stability at the cell surface.

Arf6 GTPase activates the enzyme phospholipase D, which hydrolyzes phosphatidylcholine to produce PA. Due to its geometry, PA has been postulated to be involved in the generation of negative curvature in the membrane, thus facilitating the formation and fission of vesicles (46, 47). When the production of PA was inhibited, a reduction was observed in the internalization of AChR in Chol⁻ cells, indicating that this process does indeed require PA. In other cell systems, it was demonstrated that CDx treatment stimulates PLD activity (60–62). One could speculate that PLD activation, either directly as a result of Chol depletion or indirectly via coupling to Arf6 activation, increments PA levels in membrane domains in which the AChR resides. This increment might facilitate attainment of the membrane curvature necessary for the formation of endocytic vesicles. PA may also have more specific effects. It has been proposed that AChR organizes its immediate microenvironment in the form of microdomains with higher lateral packing density and rigidity, with a possible competition between Chol and saturated PA for the same binding sites on the AChR protein (63). Furthermore, PA stabilizes the resting, agonist-activatable conformational state of the AChR (63), and this lipid is preferred to phosphatidylcholine in the immediate microenvironment of the receptor protein (64). Thus, replacement of Chol by PA in the AChR lipid microenvironment may stabilize the AChR in a conformation that is preferentially internalized by an Arf6-controlled pathway.

Fusion is an essential step during myoblast differentiation, and Arf6 has been shown to modulate C2C12 fusion by regulating PLD enzymatic activity (65). When the same dominant negative Arf6 mutant that we used in our work (Arf6T27N) was applied to myoblasts in culture, cells failed to fuse and form myotubes (66). Thus, the biological role, the *raison d'être*, of the Arf route may entail differentiation-related aspects. The AChR-expressing CHO-K1/A5 cell line developed in our laboratory and used in the present work constitutes a “minimalist” model cell system mimicking the preinnervation (aneural) embryonic stages of muscle and AChR differentiation (reviewed in Ref. 9).

Variations in Chol levels occur in muscle cell differentiation; the Chol content of BC3H-1 cells was found to be 94 ± 21 nmol of lipid/mg of protein before differentiation (*i.e.* previous to the cell surface expression of AChRs) and 124 ± 14 nmol of lipid/mg of protein in differentiated cells, when AChRs are expressed (67). Conversely, in differentiated muscle cells, Chol depletion induces the fragmentation of the relatively large, micrometer sized AChR clusters (11–14). AChR clusters are associated with highly ordered/high cholesterol membrane domains in myotubes, distinct from the more fluid surroundings (14). Diffusion of AChRs from the junctional to the perijunctional region also involves changing the Chol environment of the receptor, which may explain why perijunctional AChRs are more susceptible to internalization than junctional AChRs (51). Thus, although stabilization of AChR at the membrane is considered to occur almost exclusively as a result of specific protein-protein interactions (*i.e.* anchoring of AChR complexes to components of the cytoskeleton (68–71)), cholesterol

may not only provide the appropriate lipid microenvironment that allows these interactions to occur but also *itself* contribute as an AChR-stabilizing factor.

In conclusion, the present experiments establish that Chol levels in the membrane are important in determining the endocytic trail followed by AChR. Under Chol⁻ conditions, AChR is internalized by a pathway that depends on the activity of the small GTPases Arf6 and Rac1 and the Arf6 downstream effector phospholipase D, an internalization pathway not operative under normal Chol levels. Furthermore, under Chol⁻ conditions, receptor endocytosis no longer requires triggering by competitive antagonist (α BTX) binding or antibody cross-linking; Chol-dependent destabilization of the nanocluster organization may suffice.

Acknowledgments—We thank Drs. J. Lindstrom, S. Schmid, T. Kirchhausen, J. L. Daniotti, R. Massol, T. Kobayashi, and J. B. Cohen for gifts of reagents listed under “Experimental Procedures.”

REFERENCES

- Kumari, S., Borroni, V., Chaudhry, A., Chanda, B., Massol, R., Mayor, S., and Barrantes, F. J. (2008) *J. Cell Biol.* **181**, 1179–1193
- Karlin, A. (2002) *Nat. Rev. Neurosci.* **3**, 102–114
- Barrantes, F. J. (2003) *Curr. Opin. Drug Discov. Devel.* **6**, 620–632
- Barrantes, F. J. (2004) *Brain Res. Brain. Res. Rev.* **47**, 71–95
- Fong, T. M., and McNamee, M. G. (1987) *Biochemistry* **26**, 3871–3880
- Mayor, S., and Pagano, R. E. (2007) *Nat. Rev. Mol. Cell Biol.* **8**, 603–612
- Appel, S. H., Anwyl, R., McAdams, M. W., and Elias, S. (1977) *Proc. Natl. Acad. Sci. U.S.A.* **74**, 2130–2134
- Heinemann, S., Bevan, S., Kullberg, R., Lindstrom, J., and Rice, J. (1977) *Proc. Natl. Acad. Sci. U.S.A.* **74**, 3090–3094
- Barrantes, F. J. (2007) *J. Neurochem.* **103**, Suppl. 1, 72–80
- Borroni, V., Baier, C. J., Lang, T., Bonini, L., White, M. M., Garbus, I., and Barrantes, F. J. (2007) *Mol. Membr. Biol.* **24**, 1–15
- Willmann, R., Pun, S., Stallmach, L., Sadasivam, G., Santos, A. F., Caroni, P., and Fuhrer, C. (2006) *EMBO J.* **25**, 4050–4060
- Zhu, D., Xiong, W. C., and Mei, L. (2006) *J. Neurosci.* **26**, 4841–4851
- Stetzowski-Marden, F., Recouvreur, M., Camus, G., Cartaud, A., Marchand, S., and Cartaud, J. (2006) *J. Mol. Neurosci.* **30**, 37–38
- Stetzowski-Marden, F., Gaus, K., Recouvreur, M., Cartaud, A., and Cartaud, J. (2006) *J. Lipid Res.* **47**, 2121–2133
- Kellner, R. R., Baier, C. J., Willig, K. I., Hell, S. W., and Barrantes, F. J. (2007) *Neuroscience* **144**, 135–143
- Roccamo, A. M., Pediconi, M. F., Aztiria, E., Zanella, L., Wolstenholme, A., and Barrantes, F. J. (1999) *Eur. J. Neurosci.* **11**, 1615–1623
- Christian, A. E., Haynes, M. P., Phillips, M. C., and Rothblat, G. H. (1997) *J. Lipid Res.* **38**, 2264–2272
- Bligh, E., and Dyer, W. (1959) *Can. J. Biochem. Physiol.* **37**, 911–917
- Sato, S. B., Ishii, K., Makino, A., Iwabuchi, K., Yamaji-Hasegawa, A., Senoh, Y., Nagaoka, I., Sakuraba, H., and Kobayashi, T. (2004) *J. Biol. Chem.* **279**, 23790–23796
- St. John, P. A., and Gordon, H. (2001) *J. Neurobiol.* **49**, 212–223
- Lindstrom, J., and Einarson, B. (1979) *Muscle Nerve* **2**, 173–179
- Tzartos, S. J., Sophianos, D., Zimmerman, K., and Starzinski-Powitz, A. (1986) *J. Immunol.* **136**, 3231–3238
- Engel, A. G., and Fumagalli, G. (1982) *Ciba Found. Symp.* **90**, 197–224
- de Kruijff, B., Gerritsen, W. J., Oerlemans, A., van Dijk, P. W., Demel, R. A., and van Deenen, L. L. (1974) *Biochim. Biophys. Acta.* **339**, 44–56
- Kwik, J., Boyle, S., Fooksman, D., Margolis, L., Sheetz, M. P., and Edidin, M. (2003) *Proc. Natl. Acad. Sci. U.S.A.* **100**, 13964–13969
- Spector, I., Shochet, N. R., Kashman, Y., and Groweiss, A. (1983) *Science* **219**, 493–495
- Cooper, J. A. (1987) *J. Cell Biol.* **105**, 1473–1478
- Bubb, M. R., Spector, I., Beyers, B. B., and Fosen, K. M. (2000) *J. Biol. Chem.*

Cholesterol Modulation of AChR Endocytosis

- 275, 5163–5170
29. Bubb, M. R., Senderowicz, A. M., Sausville, E. A., Duncan, K. L., and Korn, E. D. (1994) *J. Biol. Chem.* **269**, 14869–14871
 30. Gervásio, O. L., Armson, P. F., and Phillips, W. D. (2007) *Dev. Biol.* **305**, 262–275
 31. Bruneau, E., and Akaaboune, M. (2007) *J. Biol. Chem.* **282**, 9932–9940
 32. Wang, Z. Z., Mathias, A., Gautam, M., and Hall, Z. W. (1999) *J. Neurosci.* **19**, 1998–2007
 33. Banks, G. B., Fuhrer, C., Adams, M. E., and Froehner, S. C. (2003) *J. Neurocytol.* **32**, 709–726
 34. Phillips, W. D., Vladeta, D., Han, H., and Noakes, P. G. (1997) *Mol. Cell Neurosci.* **10**, 16–26
 35. Porter, S., and Froehner, S. C. (1983) *J. Biol. Chem.* **258**, 10034–10040
 36. Porter, S., and Froehner, S. C. (1985) *Biochemistry* **24**, 425–432
 37. Benmerah, A., Bégue, B., Dautry-Varsat, A., and Cerf-Bensussan, N. (1996) *J. Biol. Chem.* **271**, 12111–12116
 38. Benmerah, A., Bayrou, M., Cerf-Bensussan, N., and Dautry-Varsat, A. (1999) *J. Cell Sci.* **112**, 1303–1311
 39. Donaldson, J. G. (2003) *J. Biol. Chem.* **278**, 41573–41576
 40. Naslavsky, N., Weigert, R., and Donaldson, J. G. (2004) *Mol. Biol. Cell.* **15**, 3542–3552
 41. D'Souza-Schorey, C., Boshans, R. L., McDonough, M., Stahl, P. D., and Van Aelst, L. (1997) *EMBO J.* **16**, 5445–5454
 42. Koo, T. H., Eipper, B. A., and Donaldson, J. G. (2007) *BMC Cell Biol.* **8**, 29
 43. Radhakrishna, H., Al-Awar, O., Khachikian, Z., and Donaldson, J. G. (1999) *J. Cell Sci.* **112**, 855–866
 44. Di Cesare, A., Paris, S., Albertinazzi, C., Dariozzi, S., Andersen, J., Mann, M., Longhi, R., and de Curtis, I. (2000) *Nat. Cell Biol.* **2**, 521–530
 45. Santy, L. C., Ravichandran, K. S., and Casanova, J. E. (2005) *Curr. Biol.* **15**, 1749–1754
 46. Siddhanta, A., and Shields, D. (1998) *J. Biol. Chem.* **273**, 17995–17998
 47. Huttner, W. B., and Schmidt, A. (2000) *Curr. Opin. Neurobiol.* **10**, 543–551
 48. Yang, S. F., Freer, S., and Benson, A. A. (1967) *J. Biol. Chem.* **242**, 477–484
 49. Nakanishi, M., Hirayama, E., and Kim, J. (2001) *Cell Biol. Int.* **25**, 971–979
 50. Zidovetzki, R., and Levitan, I. (2007) *Biochim. Biophys. Acta* **1768**, 1311–1324
 51. Akaaboune, M., Culican, S. M., Turney, S. G., and Lichtman, J. W. (1999) *Science* **286**, 503–507
 52. Brannigan, G., Hénin, J., Law, R., Eckenhoff, R., and Klein, M. L. (2008) *Proc. Natl. Acad. Sci. U.S.A.* **105**, 14418–14423
 53. Santy, L. C., and Casanova, J. E. (2001) *J. Cell Biol.* **154**, 599–610
 54. Boshans, R. L., Szanto, S., van Aelst, L., and D'Souza-Schorey, C. (2000) *Mol. Cell Biol.* **20**, 3685–3694
 55. Balasubramanian, N., Scott, D. W., Castle, J. D., Casanova, J. E., and Schwartz, M. A. (2007) *Nat. Cell Biol.* **9**, 1381–1391
 56. Grimmer, S., van Deurs, B., and Sandvig, K. (2002) *J. Cell Sci.* **115**, 2953–2962
 57. Chen, X. L., Zhang, Q., Zhao, R., Ding, X., Tummala, P. E., and Medford, R. M. (2003) *J. Pharmacol. Exp. Ther.* **305**, 573–580
 58. del Pozo, M. A., Alderson, N. B., Kiosses, W. B., Chiang, H. H., Anderson, R. G., and Schwartz, M. A. (2004) *Science* **303**, 839–842
 59. Kummer, T. T., Misgeld, T., Lichtman, J. W., and Sanes, J. R. (2004) *J. Cell Biol.* **164**, 1077–1087
 60. Diaz, O., Mébarek-Azzam, S., Benzaria, A., Dubois, M., Lagarde, M., Némoz, G., and Prigent, A. F. (2005) *J. Immunol.* **175**, 8077–8086
 61. Bobeszko, M., Krzemiński, P., Pomorski, P., Dygas, A., and Barańska, J. (2004) *Biochem. Biophys. Res. Commun.* **317**, 689–696
 62. Barabé, F., Paré, G., Fernandes, M. J., Bourgoin, S. G., and Naccache, P. H. (2002) *J. Biol. Chem.* **277**, 13473–13478
 63. Wenz, J. J., and Barrantes, F. J. (2005) *Biochemistry* **44**, 398–410
 64. Wenz, J. J., and Barrantes, F. J. (2008) *PMC Biophys.* **1**, 6
 65. Bach, A. S., Enjalbert, S., Comunale, F., Bodin, S., Vitale, N., Charrasse, S., and Gauthier-Rouvière, C. (2010) *Mol. Biol. Cell.* **21**, 2412–2424
 66. Chen, E. H., Pryce, B. A., Tzeng, J. A., Gonzalez, G. A., and Olson, E. N. (2003) *Cell* **114**, 751–762
 67. Pediconi, M. F., Politi, L. E., Bouzat, C. B., De Los Santos, E. B., and Barrantes, F. J. (1992) *Lipids* **27**, 669–675
 68. Kummer, T. T., Misgeld, T., and Sanes, J. R. (2006) *Curr. Opin. Neurobiol.* **16**, 74–82
 69. Bruneau, E. G., Brenner, D. S., Kuwada, J. Y., and Akaaboune, M. (2008) *Curr. Biol.* **18**, 109–115
 70. Huh, K. H., and Fuhrer, C. (2002) *Mol. Neurobiol.* **25**, 79–112
 71. Sanes, J. R., and Lichtman, J. W. (2001) *Nat. Rev. Neurosci.* **2**, 791–805